Scientia Iranica, Vol. 15, No. 2, pp 160–169

SCIENTIA
IRANICA

A New Wavelet-Based Approach for Internal Fault Current Identification in Power Transformers

H. Monsef* and S. Lotfifard[1]

This paper demonstrates a novel approach for the differential protection of power transformers. This method uses the Wavelet Transform (WT) and the Adaptive Network-based Fuzzy Inference System (ANFIS) to detect a fault current from an inrush current. The proposed method has been designed, based on the differences between the amplitudes of wavelet transform coefficients in a special band of frequency that is caused by faults and inrush currents. The performance of this algorithm has been simulated and tested under different conditions of the switching on of power transformers, using the PSCAD/EMTDC environment software.

INTRODUCTION

Transformers are important elements of power systems. Differential relays are commonly used for their protection and this protection system should be more reliable. This means that in non-fault situations, such as with inrush currents, it should not operate and under fault conditions, it should operate as fast as possible. Most methods for the digital differential protection of transformers are based on the harmonic content of the differential current. These methods are based on a concept, where in inrush current situations the ratio of the second harmonic of the differential current, in respect to its first component, is bigger than that of the fault current. To avoid mal-operation due to an inrush current, it is a common practice to detect the second harmonic component of the current and to block the differential protection of the power transformer, should it exceed a certain value.

A second harmonic may also be generated during internal faults on the transformers, which may be due to CT saturation, parallel capacitances or the distributed capacitances of long EHV transmission lines that are connected to the transformers and which may be greater than the second harmonic due to the inrush current [1].

In addition to current signals, voltage signals have also been used in some methods to increase the reliability of differential protection systems [2]. Yabe [3] describes a new method to discriminate internal fault from inrush current by summoning the active power flowing into transformers from each terminal. Sidhu and Sachdev [4] present a microprocessor-based identification system, which implements the algorithm that uses modal transformation to identify the magnetizing inrush and internal winding faults in three-phase transformers.

The main reason for including voltage transformers in the above-mentioned methods is the cost benefit of increased reliability in the protection system. Some other methods detect faults, based on the wave-shape fluctuations of differential currents.

Regarding the fact that the time interval between two respective peaks is smaller in an inrush current compared to a fault current, one of the methods is based on the measuring of the time interval between the respective peaks of the differential current [5]. The time of the current wave-shape being near zero is the main idea of another method [6]. The denotation of fault is time-delayed in such algorithms.

Some methods have used neural networks to identify fault conditions. In these methods, the input

*. *Corresponding Author, Center of Excellence in Applied Electromagnetic Systems, Department of Electrical Engineering, Faculty of Engineering, University of Tehran, Tehran, I.R. Iran.*

1. *Center of Excellence in Applied Electromagnetic Systems, Department of Electrical Engineering, Faculty of Engineering, University of Tehran, Tehran, I.R. Iran.*

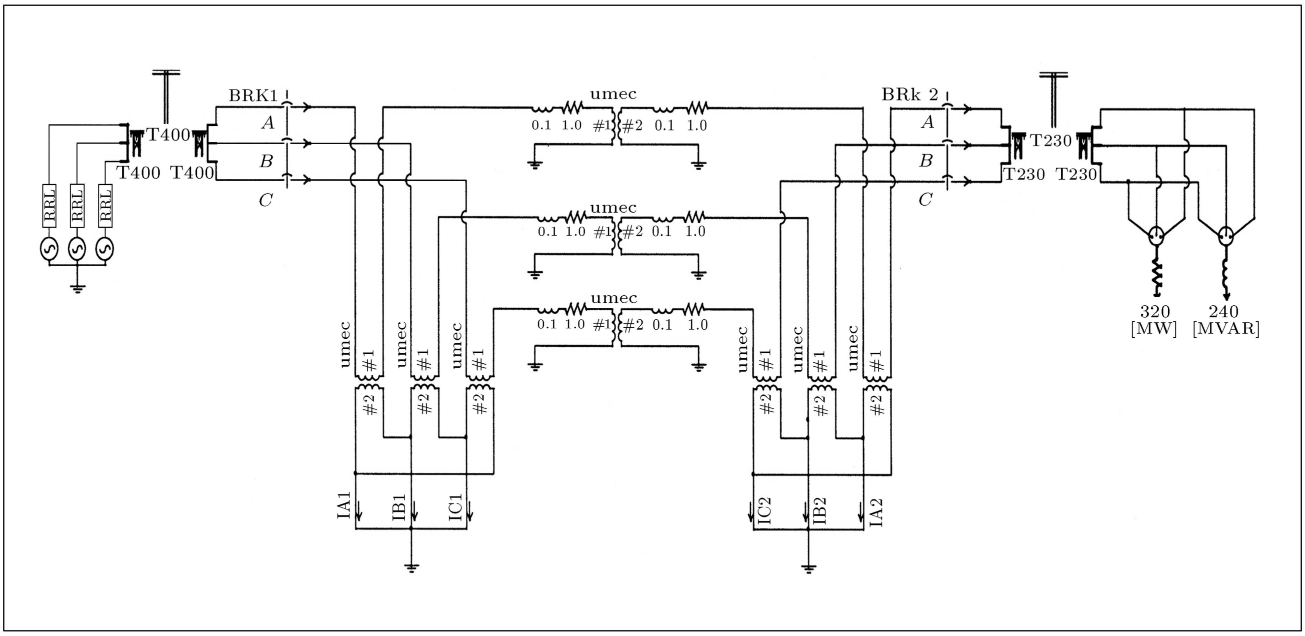

Figure 1. Sample network diagram in PSCAD environment.

of the neural network is the harmonic content of the differential current [7]. The neural network has been trained using different samples under faulted and non-faulted conditions. The trained neural network output shows the fault or the normal condition of the transformers. Some other methods use fuzzy oriented approaches, based on the harmonics of differential currents to identify the fault from an inrush current [8].

Neural network-based methods need many samples to train, which is the main deficiency of these approaches [9]. Youssef [10] presents the development of a wavelet-based scheme for distinguishing between transformer inrush and fault currents. This paper uses the distance of two respective peaks in the wavelet transform of the current for identification between fault and inrush currents.

The wavelet transform is a powerful device for assessing signals generated by transients in power systems. The main applications of a wavelet transform in a power system are: Power quality assessment [11], protection [12] and fault detection [13]. In this paper, a new approach for the differential protection of power transformers, using a fuzzy-neural network, based on a wavelet transform, has been proposed. Fuzzy logic and neural networks are powerful devices for classification and can identify faults with high reliability, but they need a lot of patterns to train. In order to solve this problem, one must extract data which contains important information as inputs of the neural network. This solution decreases the number of input patterns and quickens the identification process. For this reason, in this paper the wavelet transform is used as a reliable and fast method to decrease the number of input patterns. Consequently, the number of input samples of the system decreases to three and, hence, the learning patterns decrease considerably. The efficiency of the proposed method, with different faults and switching situations in the power transformer, has been studied. For this purpose, a small part of Iran's power system network, including a transformer that is connected to two power transmission lines, has been simulated in the PSCAD/EMTDC environment software and other elements that affect the differential current have been studied.

SAMPLE NETWORK

To study the proposed method for identifying the fault current from the inrush current in a power transformer, a part of Iran's power system network has been selected. The sample network contains a 500 MVA and 400/230 kV transformer with two current transformers that are connected to 230 kV and 400 kV lines, which are linked to the power transformer.

In this study, a detailed model of the transmission lines has been chosen. Figure 1 shows the sample network in the PSCAD/EMTDC environment.

PROPOSED METHOD FOR DISCRIMINATION BETWEEN FAULT CURRENT AND INRUSH CURRENT

It must be taken into account that the proposed method, based on the ANFIS decision, is established upon differences between wavelet transform coefficients in a special frequency band caused by the fault current and the inrush current. In this part of the paper, firstly, the wavelet transform and ANFIS have been described. Therefore, the differing behaviors of the differential current, in consequence of the fault current and the inrush current, have been characterized. Finally, a suggested technique, based on the above-mentioned characteristics, has been offered.

Wavelet Transform

The waveforms associated with fast electromagnetic transients are typically non-periodic signals, which contain both high frequency oscillations and localized impulses added to the power frequency and its harmonics. These characteristics make problems for the traditional Discrete Fourier Transform (DFT), because its usage assumes a periodic signal and the representation of a signal by the DFT is best reserved for periodic signals. As power system disturbances are subject to transient and non-periodic components, the DFT alone can be an inadequate technique for signal analysis. On the other hand, DFT can be used for stationary signals. If a signal is altered in a localized time instant, the entire frequency spectrum can be affected. To reduce the effects of non-periodic signals on the DFT, the Short-Time Fourier Transform (STFT) is used. It assumes local periodicity within a continuously translated time window. So, STFT is dependent upon time and, hence, disturbance time can be determined by it. Due to the constant value of the window width for all signals, the resolution degree of all signals is considered to be constant.

A Wavelet Transform (WT) expands a signal, not in terms of trigonometric polynomials, but by a wavelet generated using the translation (shift in time) and dilation (compression in time) of a fixed wavelet function called the mother wavelet. The wavelet function is localized in time and frequency, yielding wavelet coefficients at different scales. This gives the WT the ability to support the analysis of signals with localized transient components. The Discrete Wavelet Transform (DWT) output can be represented by a two-dimensional grid in a similar manner to the STFT, but with very different divisions in time and frequency, such that the windows are narrow at high frequencies and wide at low frequencies. In comparison with the STFT, the WT can detect transient components at the higher frequency isolated at a shorter part of the power frequency cycle. In other words, in WT, unlike STFT, the frequency spectrums are not activated all together.

The single-level decomposition process in the wavelet analysis of a signal simply consists of passing it through two complementary filters, called a Low pass Decomposition filter (LD) and a High–pass Decomposition filter (HD), and convolving the signal with filter coefficients. After this process, by down sampling the results, they come out as two components called low frequency and high frequency coefficients.

In multi-level wavelet analysis, the above mentioned single level decomposition process is iterated by successive low frequency components and, then, being decomposed in turn, so that the signal is broken down into many lower-resolution components. Figure 2 shows a four level decomposition process.

In Figure 2, the first level includes a wide band of high frequencies. If one assumes the sampling frequency of the main signal to be equal, f, then, the frequency band of the first level is $\frac{f}{4}$ to $\frac{f}{2}$, while the last level covers the lower frequencies of the signal in the narrow frequency band. Generally, the nth level of the wavelet transform comprises a frequency band of $\frac{f}{2^{n+1}}$ to $\frac{f}{2^n}$. In an opposite manner, in the time domain, the first and last levels of the wavelet transform have the smallest and largest interval times, respectively. The ability of WT to focus on upper frequency components and on small and lower frequency components at big intervals of time, can improve the analysis of signals with high frequency oscillations and localized impulses. So, a wavelet transform is suitable for the identification of wave-shape properties, transients and non-stationary signals [10].

In this paper, the sampling frequency is selected to be 2.5 kHz and the Daubechies9-db9 function is selected as the mother wavelet function [14]. The Daubechies9 function is a better frequency extractor than the Harr function. This is due to its low-pass and high-pass filters, which more resemble ideal filters than those of a Harr wavelet. On the other hand, because of its orthogonality, it satisfies the Parsaval theorem,

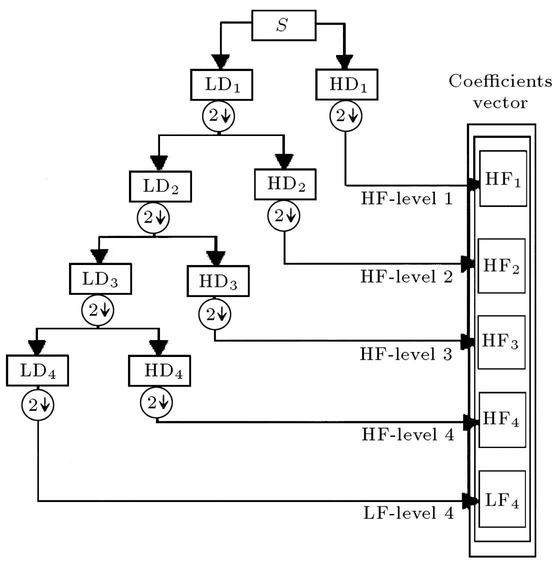

Figure 2. Four-level wavelets transform.

Table 1. Frequency band of wavelet transform coefficients.

Frequency Level	Frequency Band (Hz)
Level-D1	625-1250
Level-D2	312.5-625
Level-D3	156.25-312.5
Level-D4	78.125-312.5

unlike biorthogonal wavelets, such as Coiflet and Meyer wavelets.

The frequency components, which are confined to wavelet analysis, are according to the scheme listed in Table 1.

Fuzzy Interface System

The general scheme of a Fuzzy Inference System (FIS) has been illustrated in Figure 3 [15]. According to this figure, firstly, inputs of the system are fuzzified with membership functions. Then, a decision-making unit uses a rule-base and a data-base to make a decision in fuzzy form. Finally, the consequences of the decision-making unit are de-fuzzified and the final output is generated. There are three structures for a fuzzy decision-making unit. In this paper, the Takagi-Sugeno structure has been selected.

A Takagi_Sugeno Fuzzy Inference System with n inputs and one output is shown in Figure 4 [16]. This FIS has $n+1$ linguistic variables, n fuzzy inputs and one fuzzy output. For the system with n inputs and one output, the set of linguistic rules is defined in the form of below:

$$R_k: \text{ If } x_1 \text{ is } A_{k1} \text{ and } x_2 \text{ is } A_{k2} \ldots \text{ and } x_n \text{ is } A_{kn},$$

then:

$$f_i = p_{k1}x_1 + p_{k2}x_2 + \cdots + p_{kn}x_n + c_k,$$

where f_i is a consequence function resulted from a fuzzy rule. If all the inputs have an equal number of membership functions, such as M, then, the number of fuzzy linguistic rules will be $P = M^n$.

From Figure 4, the output from the Takagi-Sugeno FIS is as follows:

$$y = \sum_{i=1}^{p} \overline{u_i} f_i,$$

where:

$$\overline{u_i} = \frac{u_i}{\sum\limits_{i=1}^{p} u_i}, \quad \text{and} \quad u_i = \prod_{j=1}^{M} \mu_{ij}(x_j).$$

If the membership functions are taken in the Gaussian form, then:

$$\mu_{ij} = \frac{1}{1+\left[\left(\frac{x_j - a_{ij}}{c_{ij}}\right)^2\right]^{b_{ij}}}, \qquad i=1,...,n;\; j=1,...,M.$$

The consequence functions of the fuzzy rules are in the form of:

$$f_i = \sum_{j=1}^{M} p_{ij}x_j + c_i.$$

Then, from the above relations, the output of the FIS is as follows [17]:

$$y = \frac{1}{\sum\limits_{i=1}^{p} u_i} \sum_{i=1}^{p} u_i \left(\sum_{j=1}^{M} p_{ij}x_j + c_j \right).$$

In the above equations, a_{ij}, b_{ij}, c_{ij}, p_{ij} and c_j are the adapting parameters, which must be learned. ANFIS uses an iterative procedure, which is based on a decreasing gradients method. In order to learn the adapting parameters, a_{ij}, b_{ij} and c_{ij}, and the parameters of the f_i functions, p_{ij} and

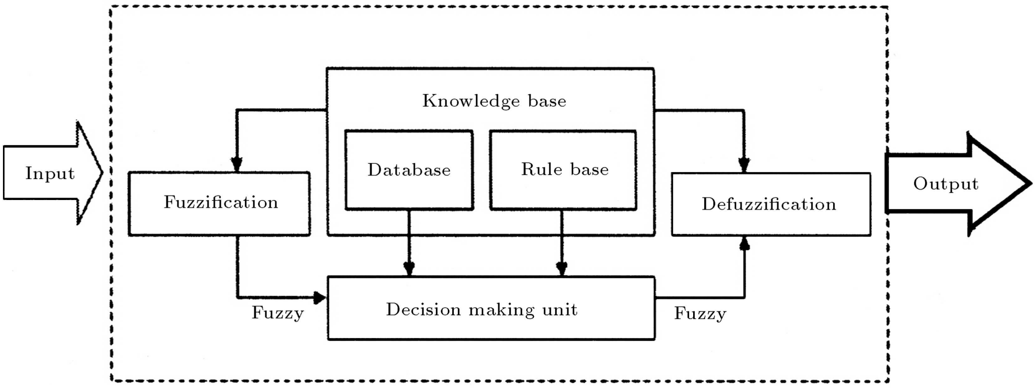

Figure 3. Fuzzy Interface System (FIS).

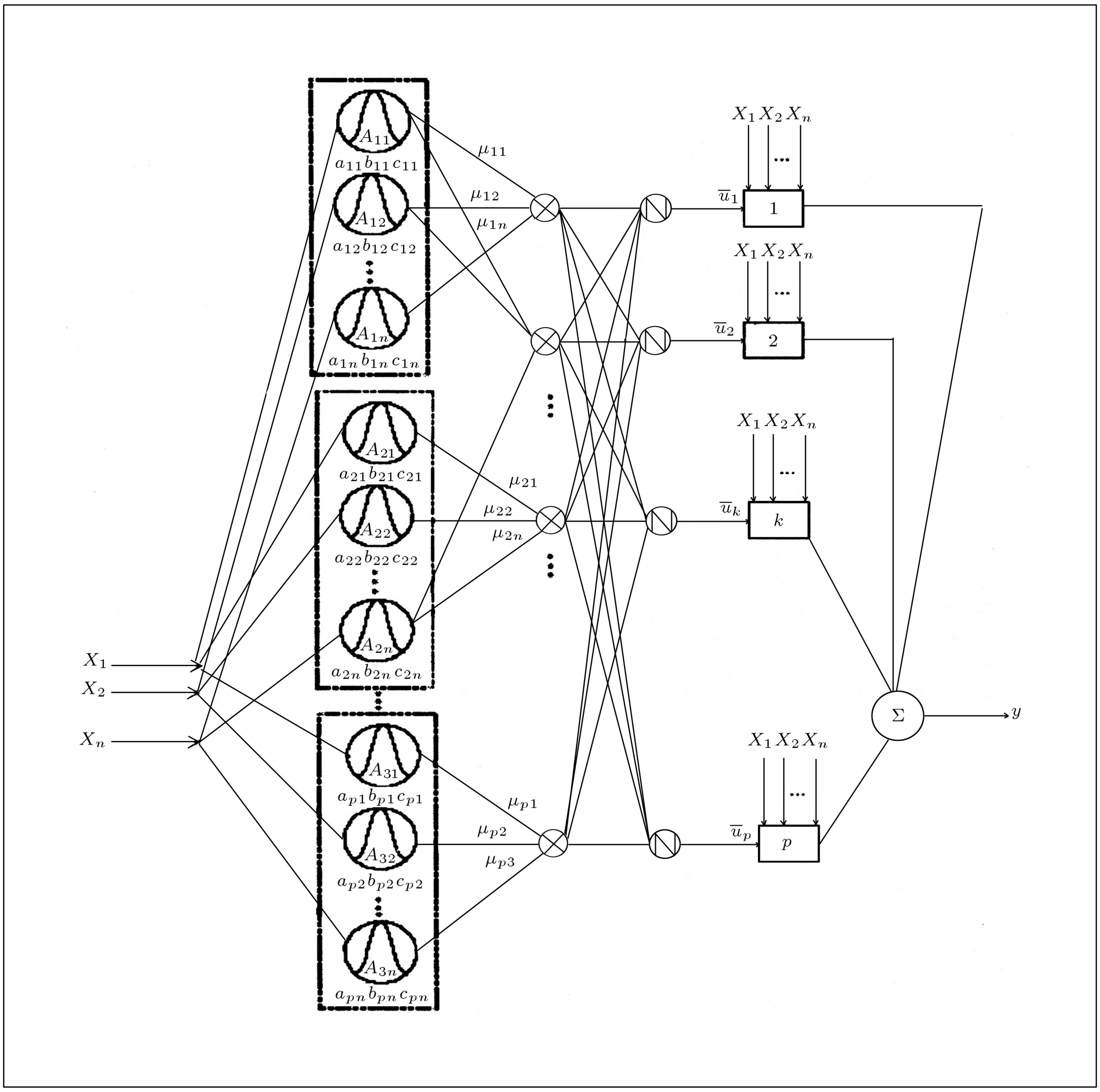

Figure 4. Fuzzy Takagi-Sugeno with n input and one output.

c_j are being adapted by the least square error method [16].

The learning procedure requires a set of data for training as $p = \{p_1, p_2, \cdots, p_r\}$. Each element of the set, $p_x = (x_k, y_{zx})$, is defined by the input vector, $x_k = (x_{1k}x_{2k}\ldots.x_{mk})$, and related response, y_{zk}.

After the learning of ANFIS, the error sum of the square is as follows [17]:

$$\varepsilon = \sum_{k=1}^{r}\left(y_{zk} - \left(\frac{1}{\sum_{i=1}^{p} u_{ik}}\sum_{i=1}^{p}\left(u_{ik}\sum_{j=1}^{M} p_{ij}x_{ij} + c_i\right)\right)\right)^2,$$

$$u_{ik} = \prod_{j=1}^{M}\mu_{ij}(x_{jk}).$$

DIFFERENTIAL CURRENT BEHAVIOR IN DIFFERENT CASES OF FAULT AND SWITCHING

Differential currents have different behaviors under fault and inrush current conditions. Since the magnetizing inrush current corresponds to the transformer core saturation, the inrush current has a conical shape (non-sinusoidal); in other words, the inrush current at the switching time increases very slowly and, as time passes, its slope increases. However, when a fault occurs, the differential current slope increases compared to the starting of the inrush current. This slope decreases as time passes. In other words, when a short circuit occurs on the transformer windings, the first and second harmonics of the differential current are increasing faster, in order to reach their maximum values, sooner than in the case of an inrush current [17].

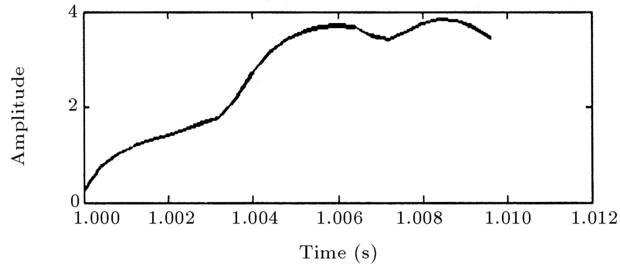

(a) Fault current

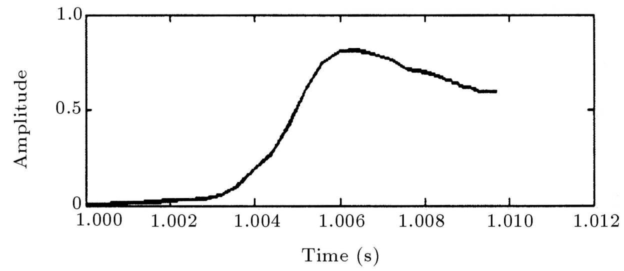

(b) Inrush current

Figure 5. (a) Fault current; and (b) Inrush current.

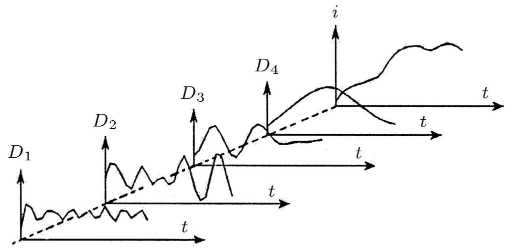

(a) Fault current

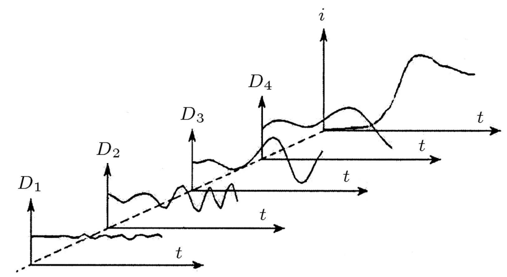

(b) Inrush current

Figure 6. Wavelet transform coefficients.

This phenomenon has been illustrated in Figure 5. Figure 5a shows the differential current of phase A due to a fault that occurs at $t = 1$ sec and continues for half of the period (0.01 sec at 50 Hz).

If an inrush current flows in the transformer windings, the differential current of the relay has a different behavior, with respect to the internal fault current. In the switching condition, in transformers, the first and second harmonics of the differential current increase, in order to reach their maximum values very slowly and after some cycles decrease with the same slope. Figure 5b illustrates the differential current of phase A of the transformer in the half cycle after switching. The differential current of phases B and C also have the same behavior as phase A.

Figures 6a and 6b show the coefficients of the wavelet transforms of the fault current and the inrush current, respectively, in diagrams D1 to D4. The amplitudes of high frequencies (frequencies which are bigger than the power frequency) in an internal fault condition are bigger than the inrush current frequencies, due to the following two reasons [17]:

- The increasing ramp rate of the fault current is bigger than the inrush current;
- The bigger ramp rates of the signals include higher frequencies in the frequency-spectrum of the signals.

These properties have been illustrated in Figures 7a and 7b for D3 in the frequencies between 156.25 Hz to 312.5 Hz , in the two cases of fault and inrush currents, respectively.

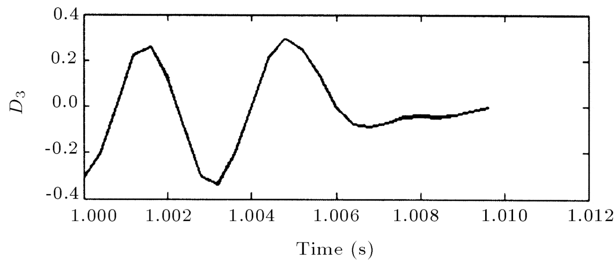

(a) Fault current

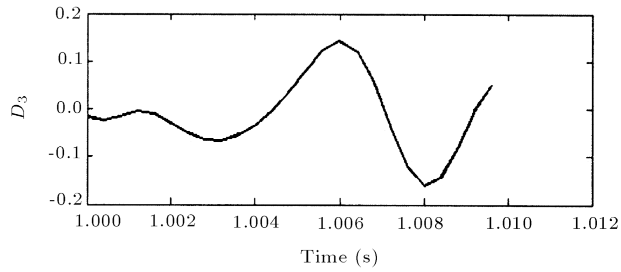

(b) Inrush current

Figure 7. Wavelet transform coefficients in D3.

For these reasons, by varying the power system or the power transformer and their parameters, the fault and inrush current wavelet transform coefficients do not change. So, these coefficients and their behavior are not affected by transformer type or power system. This property of the amplitude of the wavelet transform (such as D3) makes coefficients that can be used to identify the fault current from the inrush current. In this paper, the proposed method uses this reality.

PROPOSED APPROACH

According to the above-mentioned explanations, a set of primary data is necessary for the FIS as training patterns. Their number is highly dependent on the number of adaptive parameters, which themselves are dependent on the number of inputs. Since each Gaussian membership function has three parameters, then by this assumption, each input has an M membership function. Therefore, the number of all input parameters for n inputs is equal to: $3 * M * n$.

On the other hand, there are M^n fuzzy rules, each of which is a linear combination of inputs in addition to a constant value. Therefore, the number of parameters is equal to: $M^n(n+1)$. As a result, the number of all FIS adaptive parameters is:

$$3Mn + M^n(n+1).$$

Suppose that the consequence part of each fuzzy rule is a constant value, then the number of adaptive parameters will be reduced to:

$$3Mn + M^n.$$

It is obvious from the above that the number of parameters has an exponential relation with inputs. It means that a small variation in the number of inputs causes a large variation in the number of parameters. Table 2 shows a comparison between the number of parameters for 3, 4, 5 and 6 inputs, in which every input has three membership functions.

By increasing the number of inputs and, consequently, adaptive parameters, in addition to the need for more samples for system training, the calculation burden and algorithm response time are also increasing relatively. Therefore, the number of inputs must be decreased as much as possible, but be sufficient enough for FIS to distinguish between fault conditions and switching conditions, so that the selected input data should have the most proper information. Differences between fault and inrush currents in the D3 curves are very recognizable. In order to obtain the most proper information, the inputs have been chosen from maximum values of wavelet coefficients of D3 curves.

It is possible to find out the main reason for current wave-shape variations by the behavior of wavelet transform coefficients. This behavior is apparent in

Table 2. The number of parameters vs. the number of inputs.

No. of Parameters	No. of Inputs
54	3
117	4
288	5
748	6

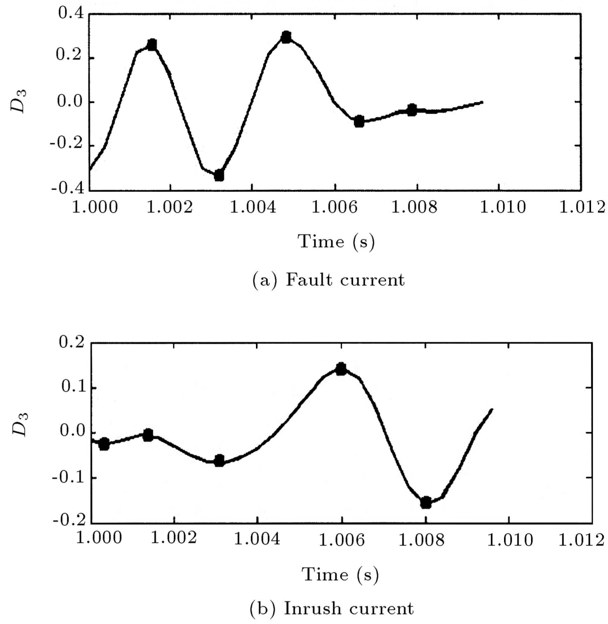

Figure 8. Peak values of wavelet transform coefficients (D3).

Figure 8. As shown in this figure, at first, the D3 curve of the fault current varies greatly and, then, its variation will be slow. In the inrush current, this behavior is opposite. Therefore, it is enough to feed the peak values of the current, in the first half cycle after the variations as input data to the FIS. Due to the fact that D3 contains a frequency band of 156.25 to 312.5, the first half-cycle of the current waveform includes 3 cycles or six peak points in the D3 curve. The first five peak points can be used as input data for the FIS. It must be a normalized current waveform, because the identification process must be independent from the amplitude of the current. To reach this aim, the maximum value of the current in the D3 curve should be selected as a base value and the other points must be divided by it. Consequently, the proposed algorithm should be based on the differences between the nature of the current under fault and safe conditions and not be established upon the magnitude of the current. As a result, the maximum value of the current in the D3 curve is equal to one in all cases and, so it can be removed from the set of five input data. Hence, the number of inputs decreases to four. On the other hand, because the algorithm is based on the differences between the current magnitudes, by calculating the difference values, one of the inputs can be omitted without reducing the abilities of the proposed algorithm. Finally, the number of input data will be equal to 3 and the number of FIS training parameters is equal to 54. After FIS training, the final error of the training process is 0.017. Figure 9 shows this fact.

It must be taken into account that the output

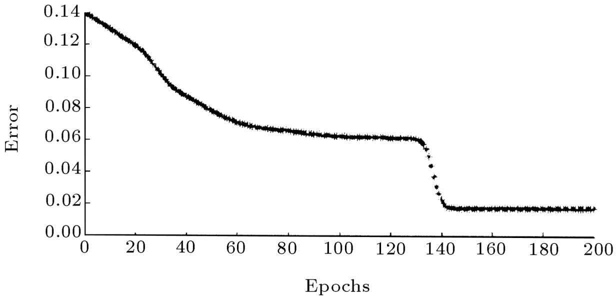

Figure 9. Training process error.

of the FIS is a real number, but the desirable output is 1 or 0 (1 means the fault and 0 means the safe condition). So, if the output of the FIS is near 1, the final output is rounded to 1, else it is rounded to 0. According to this strategy, the final output of the FIS, with high accuracy, can determine fault and safe situations.

Results of the Proposed Algorithm Implementation

In order to assess the efficiency of the proposed algorithm, different cases of fault current and inrush current have been simulated. These case studies have been accomplished by changing the main parameters that have an influence on inrush current properties. These parameters are:

- Magnitude of residual flux in the transformer core of each phase (Br),
- Voltage angle of phase A (when switching occurred on it),
- Switching of transformer with secondary windings open or closed,
- Knee point voltage of the saturation curve of the transformer core,
- Amplitude of voltage connected to the transformer.

Different cases of fault current have been simulated by considering the main parameters to affect the characteristics of the current.

The results of implementing the proposed algorithm for different cases have been shown in Table 3.

Table 3 shows the output of ANFIS for different phases in the half-cycle after current variations, due to inrush current. The first column of this table shows the amplitudes of the residual flux in the transformer core for each phase in the switching condition with respect to nominal flux. The voltage angle of phase A has been mentioned in the second column of this table. The third column of the table determines the differential current pertaining to whichever phase. The fourth and fifth columns show that when the inrush current flows in the transformer windings, the secondary windings of the transformer is open or closed.

Table 3. Output of ANFIS in the half period of time after switching for different amounts of inrush current.

B_r	Θ_A	Phase	No-Load Case				Loading Case			
			Stiff System		Weak System		Stiff System		Weak System	
			Property Curve #1	Property Curve #2	Property Curve #1	Property Curve #2	Property Curve #1	Property Curve #2	Property Curve #1	Property Curve #2
$B_{rA}=0$ $B_{rB}=0$ $B_{rC}=0$	0	A	-0.060	0.0234	0.086	0.0054	-0.002	0.1782	0.0128	0.0094
		B	0.1705	0.001	-0.004	0.1471	0.0341	0.003	-0.007	0.1382
		C	0.0547	0.023	0.2413	0.0912	0.00812	0.153	0.0972	0.0032
	72	A	0.020016	0.0845	0.0905	0.005	0.008	0.0529	0.1942	0.0541
		B	-0.13011	0.0032	0.009	0.001	0.01903	0.1451	0.004	0.112
		C	0.025102	-0.002	0.0458	0.119	0.0115	0.008	0.1283	0.0041
$B_{rA}=55\%$ $B_{rB}=0$ $B_{rC}=-55\%$	0	A	0.0012076	0.2015	0.1005	-0.029	0.2001	0.0114	0.001	0.0927
		B	-0.036514	0.0021	0.001	0.004	0.00917	0.1762	0.0971	0.0038
		C	0.020874	0.07301	0.08492	0.1831	0.115	0.1448	0.186	-0.023
	72	A	0.1423	0.2361	0.2063	0.0047	0.007	0.0021	0.1824	0.0045
		B	0.0263	0.1494	0.001	0.0083	0.0154	0.0819	0.0051	0.0871
		C	0.001	-0.0317	0.0719	0.018	0.0318	0.0351	0.0035	0.0627

Table 4. Output of ANFIS in the half period of time for different cases of fault situation.

Θ_A	Phase	No-Load Case				Loading Case			
		a-g	**a-b**	**a-b-c**	**a-b-g**	**a-g**	**a-b**	**a-b-g**	**a-b-c**
0	A	0.99894	0.99878	0.95985	0. 98947	1.0512	0.9519	1.003	0.9865
	B	0.98949	0.99169	0.98418	0.98950	1.0404	1.0398	0.9976	0.9759
	C	1.0000	1.0005	0.98435	0. 98427	1	0.9998	0.9957	0.9932
72	A	0.98751	0.99653	0. 98426	1.002	0.7958	0.994	1.008	0.9984
	B	1.0099	0. 99029	0. 99901	0.987	0.9959	0.9855	0.9963	1.006
	C	1.0098	1.001	0. 97352	0.9978	0.9961	0.9913	0.9914	0.9925

The effect of the flux density at the knee point in the saturation curve of the transformer core, under no load and loading conditions of the transformer, has been studied. The flux density amplitude of the knee point in the second characteristic curve of the core is larger than that of the first. The result of implementing the proposed algorithm for fault current conditions has been presented in Table 4.

In addition to the fault current and inrush current conditions, it is necessary to study the performance of the proposed algorithm when fault occurs under switching conditions. Table 5 shows the four different states of the transformer when internal fault and switching have occurred, simultaneously. The first and second rows of this table present different states of switching conditions.

Indices ij in these two rows means that it belongs to the ith row of Table 3 and the jth column of Table 4. The results of Tables 3, 4 and 5 all show that the proposed algorithm operates correctly.

CONCLUSION

In this paper, a novel approach for the differential protection of a power transformer has been presented. This approach is based on the differences between the amplitudes of wavelet transform coefficients in the special frequency band, caused by fault current and inrush current. In this method, the output of the ANFIS decision system shows the internal fault or the inrush current conditions of the transformer. If its output is equal to 1, it shows the fault condition; otherwise switching has occurred in the transformer.

Table 5. Output of ANFIS in the half period of time after simultaneous occurrence of fault and switching conditions.

Switching Situation	1,1	2,4	3,6	4,7
Fault Situation	1,1	2,4	1,6	2,7
A	1.004	0.9947	0.9918	0.9964
B	0.9891	1.007	0.9864	1.011
C	0.9714	1.003	0.9827	0.9912

The proposed algorithm besides being highly accurate is also extremely fast. The decision making process of this method is based on three samples and the proposed algorithm can detect a fault current from an inrush current in less than a half-cycle of time. Another advantage of this approach is in the fewer number of patterns required for training ANFIS. The efficiency of this method has been simulated under different conditions of internal fault and switching. The results of the studies show that the proposed algorithm is suitable for the differential protection of power transformers.

REFERENCES

1. Lio, P., Malik, O.P., Chen, C., Hope, G.S. and Guo, Y. "Improved operation of differential protection of power transformer for internal faults", *IEEE Trans. on Power Delivery*, **7**(4), pp 1912-1919 (1992).
2. Inagaki, K. and Higaki, M. "Digital protection method for power transformers based on an equivalent circuit composed of inverse inductance", *IEEE Trans. on Power Delivery*, **3**(4), pp 1501-1510 (1998).
3. Yabe, K. "Power differential method for discrimination between fault and magnetizing inrush current in transformers", *IEEE Trans. on Power Delivery*, **12**(3), pp 1109-1117 (1997).
4. Sidhu, T.S. and Sachdev, M.S. "On line identification of magnetizing inrush and internal faults in three phase transformers", *IEEE Trans. on Power Delivery*, **7**(4), pp 1885-1890 (1992).
5. Rockefeller, G.D. "Fault protection with a digital computer", *IEEE Trans. on PAS.*, **-PAS-98**, pp 438-464 (1969).
6. Giuliante, A. and Clough, G. "Advances in the design of differential protection for power transformers", *Georgia Technical Protective Relaying Conference*, Atlanta, Georgia, pp 1-12 (May 1-3 1991).
7. Bastard, P., Meunier, M. and Regal, H. "Neural network-based algorithm for power transformer differential relays", *IEE Proceedings C*, **142**(4), pp 386-392 (1995).
8. Wiszniewski, A. and Kasztenny, B. "A multi-criteria differential transformer relay based on fuzzy logic",

IEEE Trans. on Power Delivery, **10**(4), pp 1786-1792 (1995).

9. Hamedani Golshan, M.E., Saghaian-nejad, M., Saha, A., Samet, H. "A new method for recognizing internal faults from inrush current conditions in digital differential protection of power transformer", *Electric Power Systems Research*, **71**, pp 61-67 (2004).
10. Youssef, O.A.S. "A wavelet-based technique for discrimination between fault and magnetizing inrush currents in transformers", *IEEE Trans. on Power Delivery*, **18**(1), pp 170-176 (Jan. 2003).
11. Santoso, S., Powers, E.J., Grady, W.M. and Hofmann, P. "Power quality assessment via wavelet transforms analysis", *IEEE Trans. on Power Delivery*, **11**(2), pp 924-930 (Apr. 1996).
12. Chaari, O., Meunier, M. and Brouaye, F. "Wavelets: A new tool for the resonant grounded power distribution systems relaying", *IEEE Trans. on Power Delivery*, **11**(3), pp 1301-1308 (July 1996).
13. Jiang, F., Bo, Z.Q. and Redfern, M.A. "A new generator fault detection scheme using wavelet transform", *Proc. 33rd Univ. Power Eng. Conf., Edinburgh*, UK, pp 360-363 (Sept. 1998).
14. Daubechies, I., *Ten Lectures on Wavelets*, SIAM, Philadelphia, Pennsylvania (1992).
15. Ranković, V. "Application of the Takagi-Sugeno fuzzy controller for solving the robots' inverse kinematics problem", *Mechanics, Automatic Control and Robotics*, **3**(15), pp 1039-1054 (2003).
16. Jang, S.R. "ANFIS: Adaptive-network-based fuzzy inference system", *IEEE Trans. on Systems, Man and Cybernetics*, **23**(3), pp 665-685 (1993).
17. Guzman, A. "Performance analysis of traditional and improved transformer differential protective relays", *SEL Technical Papers*, pp 405-412 (2000).